CHRONIC ITCH

Gate control of mechanical itch by a subpopulation of spinal cord interneurons

Steeve Bourane,[1]* Bo Duan,[2]* Stephanie C. Koch,[1] Antoine Dalet,[1] Olivier Britz,[1] Lidia Garcia-Campmany,[1] Euiseok Kim,[3] Longzhen Cheng,[2,4] Anirvan Ghosh,[3] Qiufu Ma,[2]† Martyn Goulding[1]†

Light mechanical stimulation of hairy skin can induce a form of itch known as mechanical itch. This itch sensation is normally suppressed by inputs from mechanoreceptors; however, in many forms of chronic itch, including alloknesis, this gating mechanism is lost. Here we demonstrate that a population of spinal inhibitory interneurons that are defined by the expression of neuropeptide Y::Cre (NPY::Cre) act to gate mechanical itch. Mice in which dorsal NPY::Cre-derived neurons are selectively ablated or silenced develop mechanical itch without an increase in sensitivity to chemical itch or pain. This chronic itch state is histamine-independent and is transmitted independently of neurons that express the gastrin-releasing peptide receptor. Thus, our studies reveal a dedicated spinal cord inhibitory pathway that gates the transmission of mechanical itch.

The sensation of itch elicits stereotypical scratching behaviors that are an important protective response to cutaneous irritants and parasites. Animals appear to have evolved two forms of itch: (i) chemical itch, which is activated by chemical mediators such as histamines and proteases (*1*–*6*) and can be effectively gated by noxious painful stimuli (*7*), and (ii) mechanical itch, which is evoked by light tactile stimuli, such as when insects or parasites come in contact with the skin. In humans, this latter pathway can be activated by vibrating the fine vellous hair (*8*). Itching is also frequently evoked by light mechanical stimuli in patients suffering from chronic itch (*9*, *10*).

Although progress has been made toward identifying the spinal inhibitory neurons that gate chemical itch (*11*, *12*), little is known about the spinal pathways gating mechanical itch. The dorsal horn of the spinal cord contains multiple inhibitory interneuron (IN) populations including cells that express neuropeptide Y (NPY) (*13*, *14*). These cells are distinct from those that express dynorphin, galanin, neuronal nitric oxide synthase (nNOS), and parvalbumin (*15*, *16*). When *NPY::Cre* transgenic mice [Gene Expression Nervous System Atlas (GENSAT), RH26 cell line (see supplementary materials and methods)] were crossed with *R26*$^{\text{LSL-tdTomato}}$ (*ai14*) reporter mice to trace the provenance of the dorsal horn INs expressing NPY, NPY::Cre-derived INs were localized in laminae III and IV (70.4 ± 0.3%) and, to a lesser extent, in laminae I and II (29.6 ± 0.3%) (Fig. 1, A and B). The number of NPY$^+$/tdTomato$^+$ INs decreases postnatally, with only 35% of the tdTomato cells expressing NPY at postnatal day 30 (P30) (Fig. 1C). NPY::Cre thus captures two populations of NPY-expressing neurons: one that transiently expresses NPY during late embryonic and early neonatal development

[1]Molecular Neurobiology Laboratory, The Salk Institute for Biological Studies, 10010 North Torrey Pines Road, La Jolla, CA 92037, USA. [2]Dana-Farber Cancer Institute and Department of Neurobiology, Harvard Medical School, 1 Jimmy Fund Way, Boston, MA 02115, USA. [3]Neurobiology Section, Division of Biological Sciences, University of California, San Diego, CA 92093, USA. [4]Institute of Brain Science and State Key Laboratory of Medical Neurobiology, Fudan University, Shanghai 200032, China.
*These authors contributed equally to this work.
†Corresponding author. E-mail: goulding@salk.edu (M.G.); qiufu_ma@dfci.harvard.edu (Q.M.)

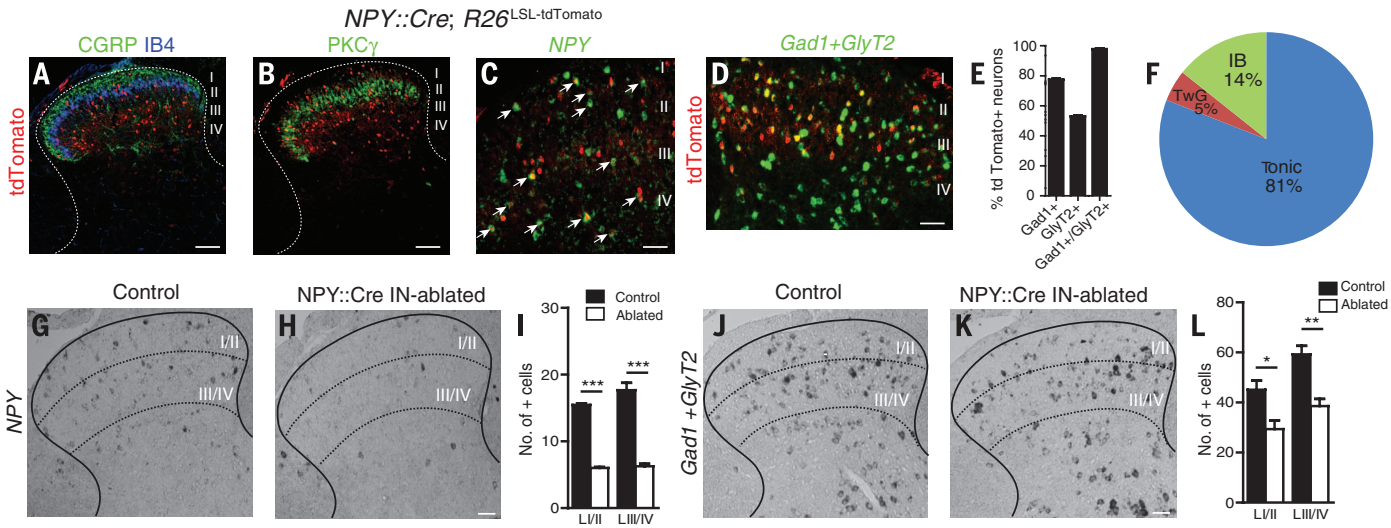

Fig. 1. NPY::Cre delineates a population of inhibitory neurons in the dorsal spinal cord. (**A** and **B**) Sections through the lumbar dorsal spinal cord of a P30 *NPY::Cre*; *R26*$^{\text{LSL-tdTomato}}$ mouse stained with calcitonin gene-related peptide (CGRP) and IB4 (A) and protein kinase Cγ (PKCγ) (B). tdTomato$^+$ fluorescence was visualized without staining. Roman numerals denote laminae. (**C**) A section through the lumbar dorsal spinal cord of a P30 *NPY::Cre*; *R26*$^{\text{LSL-tdTomato}}$ mouse, comparing expression of tdTomato reporter (red) and NPY (green, in situ). Arrows indicate double-labeled cells. (**D**) A section through the lumbar dorsal horn of a P30 *NPY::Cre*; *R26*$^{\text{LSL-tdTomato}}$, showing coexpression of tdTomato with the inhibitory markers *Gad1* and *GlyT2*. (**E**) Quantification of coexpression of NPY-tdTomato$^+$ with Gad1-GFP, GlyT2-GFP, and Gad1$^+$/GlyT2 in situ hybridization. (**F**) Firing properties of NPY::Cre INs. The majority of NPY-tdTomato$^+$ INs (34 of 42 cells) display a tonic firing pattern upon current injection. IB, intermittent bursting; TwG, tonic firing with gap. (**G** to **L**) In situ analysis and quantification of NPY [(G) to (I)] and Gad1/GlyT2 [(J) to (L)] expression in the lumbar dorsal spinal cord of P60 control and NPY::Cre IN–ablated mice. NPY$^+$ cell numbers were reduced by 59.0 and 69.5% in laminae I and II and laminae III and IV, respectively [(I) ***$P < 0.001$]. Gad1$^+$ and GlyT2$^+$ cell numbers were reduced by 34.7% in laminae I and II [(L) *$P < 0.05$] and 34.9% in laminae III and IV [(L) **$P < 0.01$]. *P* values were calculated using the Student's unpaired *t* test. Scale bars: 50 μm [(C), (D), (H), and (K)]; 200 μm [(A) and (B)]. Error bars indicate SEM [(I) and (L)].

and another that shows persistent expression into adulthood.

More than 98% of the NPY::Cre-tdTomato^{+} cells expressed glutamic acid decarboxylase 1 (Gad1) and/or the glycine transporter 2 (GlyT2^{+}) (Fig. 1, D and E). After current injection, the majority of cells (34 of 42) displayed a tonic firing pattern (Fig. 1F) that is characteristic of many dorsal horn inhibitory INs (*17*). These NPY::Cre INs make up 31 and 45% of the inhibitory Gad1^{+} or GlyT2^{+} INs in laminae I and II, and in laminae III and IV, respectively. Very few of the NPY::Cre INs cells expressed nNOS (4.9 ± 0.6%), galanin (5.0 ± 1.1%), dynorphin (8.2 ± 1.6%), or parvalbumin (5.9 ± 1.7%), indicating that they constitute a distinct population of dorsal horn inhibitory INs.

An intersectional genetic strategy that restricts diphtheria toxin receptor (DTR) expression to NPY::Cre-derived INs in the dorsal spinal cord and medulla (*18*) was then used to determine the contribution the NPY::Cre INs make to gating cutaneous sensory stimuli. Injecting *NPY::Cre; Lbx1*^{FlpO}; *Tau*$^{ds\text{-}DTR}$ mice with diphtheria toxin (DTX) markedly reduced the number of NPY::Cre-tdTomato INs in the dorsal spinal cord (fig. S1, A to C). This cell loss was restricted to inhibitory INs that express NPY, Gad1 and/or GlyT2 (Fig. 1, G to L, and fig. S1, G to I), and Pax2 (fig. S1, D to F). Neighboring dorsal inhibitory IN subtypes expressing nNOS, dynorphin, and parvalbumin (fig. S1, J to R) were spared, as were dorsal excitatory IN subtypes (fig. S2, A to L). There was no noticeable change in the central projections of sensory afferent nerve fibers or in the distribution of NPY::Cre-derived neurons in other regions of the central nervous system (fig. S3, A and B).

Two weeks after injection with DTX, the NPY::Cre IN–ablated mice began to display spontaneous scratching, followed by the appearance of skin lesions (Fig. 2, A and B). This scratching was not related to chemical itch, as injection of chemical pruritogens (compound 48/80 and chloroquine) into the nape region of NPY::Cre IN–ablated mice before the onset of spontaneous scratching revealed no difference in the level or intensity of scratching (Fig. 2, C and D). Following a modified protocol for analyzing alloknesis in mice in which von Frey hairs were used to deliver graded mechanical forces to the nape of the neck (*19*) (Fig. 2E), we observed a significant increase in evoked hindlimb scratching in NPY::Cre IN–ablated mice with low-force (0.02 to 0.4 g) von Frey hairs as compared with control mice (Fig. 2F). In contrast, high-threshold mechanical stimuli (0.6 to 1 g) did not induce pronounced scratching. Additional behavioral tests revealed no marked differences between control and NPY::Cre IN–ablated mice with regard to their responsiveness to noxious mechanical and thermal stimuli (fig. S4A). Acute chemical pain sensitivity was also normal: Injection of capsaicin into the cheek of control and NPY::Cre IN–ablated mice produced similar levels of pain-indicating wiping, with little or no itch-indicating scratching (*20*) (fig. S4B).

To rule out the possibility that the increased scratching in NPY::Cre IN–ablated mice arises from secondary changes to the spinal circuitry after neuronal ablation, we used an intersectional genetic strategy—which involves mice that carry a conditional double-stop allele encoding the inhibitory hM4D DREADD receptor (*21*) (*R26*$^{ds\text{-}hM4D\text{-}tdTomato}$) (fig. S5, A and B)—to acutely silence the NPY::Cre-derived INs (Fig. 2G). Activation of hM4D with clozapine *N*-oxide (CNO) precipitated a mechanical itch phenotype that closely resembled the itching behavior observed after NPY::Cre IN ablation (Fig. 2H). Forty min after CNO injection, low-threshold mechanical

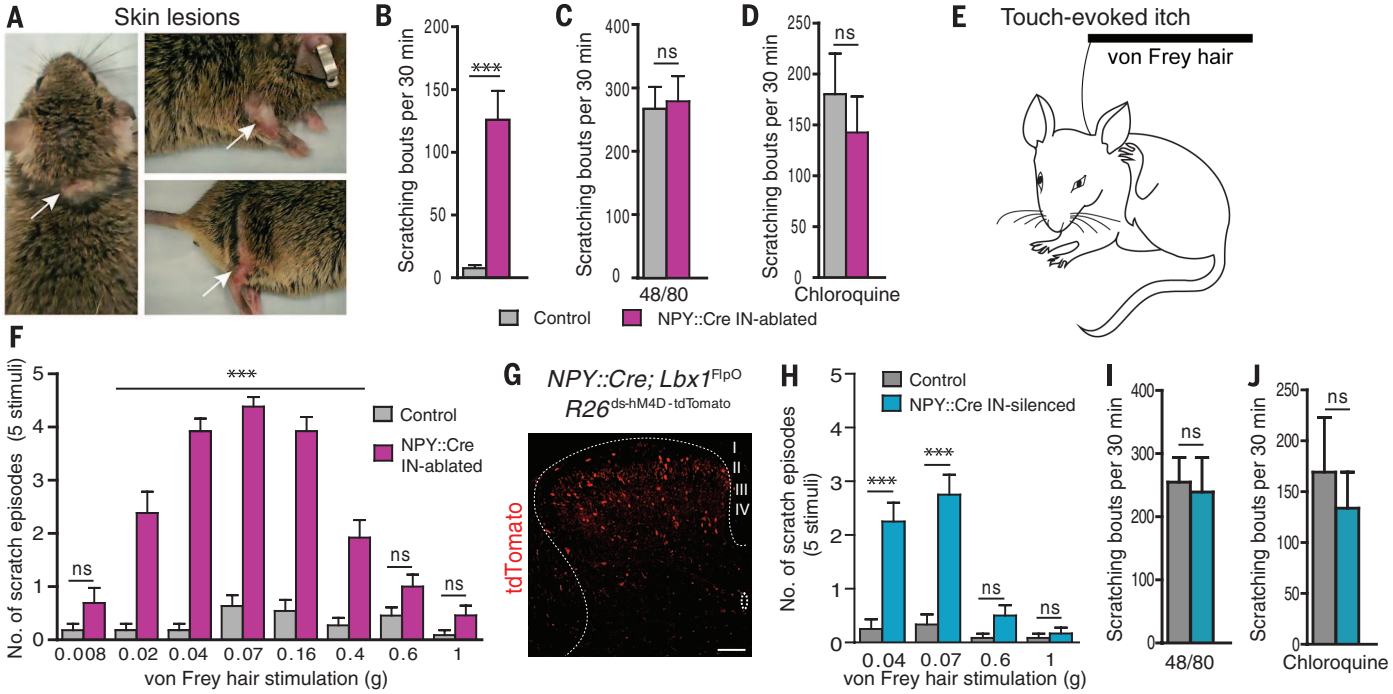

Fig. 2. Ablation or silencing of NPY::Cre INs induces touch-evoked itch. (**A**) Skin lesions on the neck and body of NPY::Cre IN–ablated mice 2 weeks after injection with DTX. (**B**) Number of spontaneous scratch events over a 30-min period (control: 7.5 ± 2.6; NPY::Cre IN–ablated: 125.8 ± 23.2; n = 10 mice; ***P < 0.001). (**C** and **D**) Equivalent responses to chemical-evoked itch are seen in control and NPY::Cre IN–ablated mice 7 days after DTX injection and before development of the spontaneous scratch phenotype. (C) Compound 48/80 (control: 266.8 ± 34.9; NPY::Cre IN–ablated: 279 ± 39.6; n = 6 mice; P = 0.82). (D) Chloroquine (control: 180.1 ± 39.8, n = 7 mice; NPY::Cre IN–ablated: 142.5 ± 35.3, n = 6 mice; P = 0.50). (**E**) Schematic showing the touch-evoked itch (alloknesis) test. (**F**) Increase in the number of scratch events after applying von Frey hairs to the shaved nape of the neck (control: n = 11 mice; NPY::Cre IN–ablated: n = 13 mice; ***P < 0.001). (**G**) tdTomato reporter expression in a section through the lumbar dorsal spinal cord of *NPY::Cre*; *Lbx1*^{Flpo}; *R26*$^{ds\text{-}hM4D\text{-}tdTomato}$ mice. Scale bar, 200 μm. (**H**) An increase in the number of scratches associated with low-intensity force (0.04 and 0.07 g), but not high-intensity force (0.6 and 1 g), is seen in NPY::Cre IN–silenced mice compared with control mice (control: n = 12 mice; NPY::Cre IN–silenced: n = 12 mice; ***P < 0.001). (**I** and **J**) Equivalent responses to chemical-evoked itch are seen in control and NPY::Cre IN–silenced mice. (I) Compound 48/80 (control: 254.8 ± 39.03; NPY::Cre IN–silenced: 239 ± 54.78; n = 6 mice; P = 0.82). (J) Chloroquine (control: 169.3 ± 53.6, n = 6 mice; NPY::Cre IN–silenced: 133.9 ± 35.49, n = 7 mice; P = 0.58). ns, no significant difference. P values were calculated using the Student's unpaired t test. Error bars indicate SEM [(B) to (D), (F), and (H) to (J)].

stimuli (0.04 and 0.07 g) produced robust scratching, whereas high-threshold mechanical stimuli (0.6 and 1 g), which typically produce pain, did not. Silencing the NPY::Cre INs did not increase scratching behavior after exposure to compound 48/80 and chloroquine (Fig. 2, I and J). Responses to von Frey hairs, brush stroke, and the Hargreaves test were also unchanged (fig. S5C), and there was no increase in mechanical allodynia after injection with Freund's complete adjuvant (fig. S5, D and E), which indicates that NPY::Cre-derived INs primarily inhibit mechanical itch.

Dorsal horn neurons that express the gastrin-releasing peptide receptor (GRPR) are required for itch transduction by a variety of chemical pruritogens (*22*, *23*). To address whether the mechanical itch pathway gated by the NPY::Cre INs differs from this chemical itch pathway, chemical itch was blocked either pharmacologically or by ablating the GRPR neurons in the dorsal horn. As compared with saline-treated controls, NPY::Cre IN–ablated mice treated with a H1/H4 histamine receptor antagonist displayed no reduction in the number of scratch events after mechanical stimulation on the nape of the neck (Fig. 3A), despite the antagonist being highly effective in reducing compound 48/80–induced scratching (Fig. 3B). Although intrathecal injection of a GRPR antagonist or ablation of GRPR-expressing neurons with conjugated bombesin-saporin (fig. S6) was effective in blocking chloroquine-evoked itch (*22*) (Fig. 3, D and F), these manipulations failed to blunt scratching in response to mechanical stimulation in NPY::Cre IN–ablated mice (Fig. 3, C and E). Mechanical itch gated by NPY::Cre INs is therefore independent of the histaminergic and GRP-GRPR itch pathways described to date (*1*–*7*).

To assess whether the NPY::Cre INs contribute to the tactile inhibition of itch, we asked if the NPY::Cre INs are innervated by cutaneous low-threshold mechanoreceptors (LTMs). In *Pitx2-EGFP* mice (GENSAT; EGFP, enhanced green fluorescent protein), myelinated hair follicle afferent fibers that selectively express GFP (fig. S7, A to C) form multiple contacts on the cell bodies and dendrites of NPY::Cre INs (Fig. 4, A and B). When cholera toxin B (CTB) was injected into the hairy skin (fig. S7, D to G) (*24*), presumptive CTB^+/$vGluT1^+$ Aβ- and Aδ-LTM synaptic boutons and putative CTB^+/$vGluT1^-$ C-LTM synaptic contacts were detected on NPY::Cre-tdTomato$^+$ INs in laminae III and IV (Fig. 4C and fig. S7Ga, arrows) and lamina II (Fig. 4C and fig. S7Gb), respectively. The synaptic nature of these contacts was confirmed by single-synapse transsynaptic rabies tracing (Fig. 4, D to G, and fig. S7, H to J) and whole-cell recordings from NPY::Cre-tdTomato neurons (Fig. 4H). Our demonstration that the NPY::Cre INs receive LTM inputs, coupled with evidence from humans that mechanical itch is gated by LTMs (*8*), suggests that NPY::Cre INs mediate the tactile inhibition of mechanical itch.

We next examined how neurons in laminae I to III respond to innocuous touch (brush stroke) (Fig. 4, I and J) and painful stimuli (pinch) (fig. S8, B and C) after NPY::Cre IN ablation. Neurons with hairy-skin receptive fields displayed a significant increase in afterdischarge spike number in NPY::Cre IN–ablated mice compared with control mice (Fig. 4I). This occurred in the absence of any concomitant increase in spontaneous activity (fig. S8A). In contrast, afterdischarge activity was unchanged following brush stroke in neurons with glabrous-skin receptive fields (Fig. 4J) or noxious stimulation (pinch) of both hairy and glabrous skin (fig. S8, B and C). Therefore, NPY::Cre INs have a specific role in gating innocuous mechanosensory inputs from hairy skin. This finding is consistent with our observation that scratching and skin lesions are restricted to hairy sites in NPY::Cre IN–ablated mice (Fig. 2A), and sensitivity to noxious or mechanical stimulation on the glabrous skin is unchanged (fig. S4).

Our findings reveal that inhibitory spinal INs marked by the expression of NPY::Cre selectively gate low-threshold mechanical itch. In contrast, *Bhlhb5* conditional knockout mice show increased sensitivity to chemical itch (*11*). NPY expression is not affected in the *Bhlhb5* mutant cord (*17*), and several Bhlhb5-dependent inhibitory IN subtypes are spared after NPY::Cre IN ablation (fig. S1). This suggests that NPY::Cre-derived and Bhlhb5-dependent inhibitory INs are required to gate mechanical and chemical itch pathways, respectively (summarized in Fig. 4K). The loss of NPY::Cre INs (fig. S4) or Bhlhb5-dependent inhibitory INs (*11*) does not affect mechanical pain, which is gated by dynorphin-expressing inhibitory INs (*18*). Therefore, inhibitory INs in the dorsal horn appear to be organized into discrete

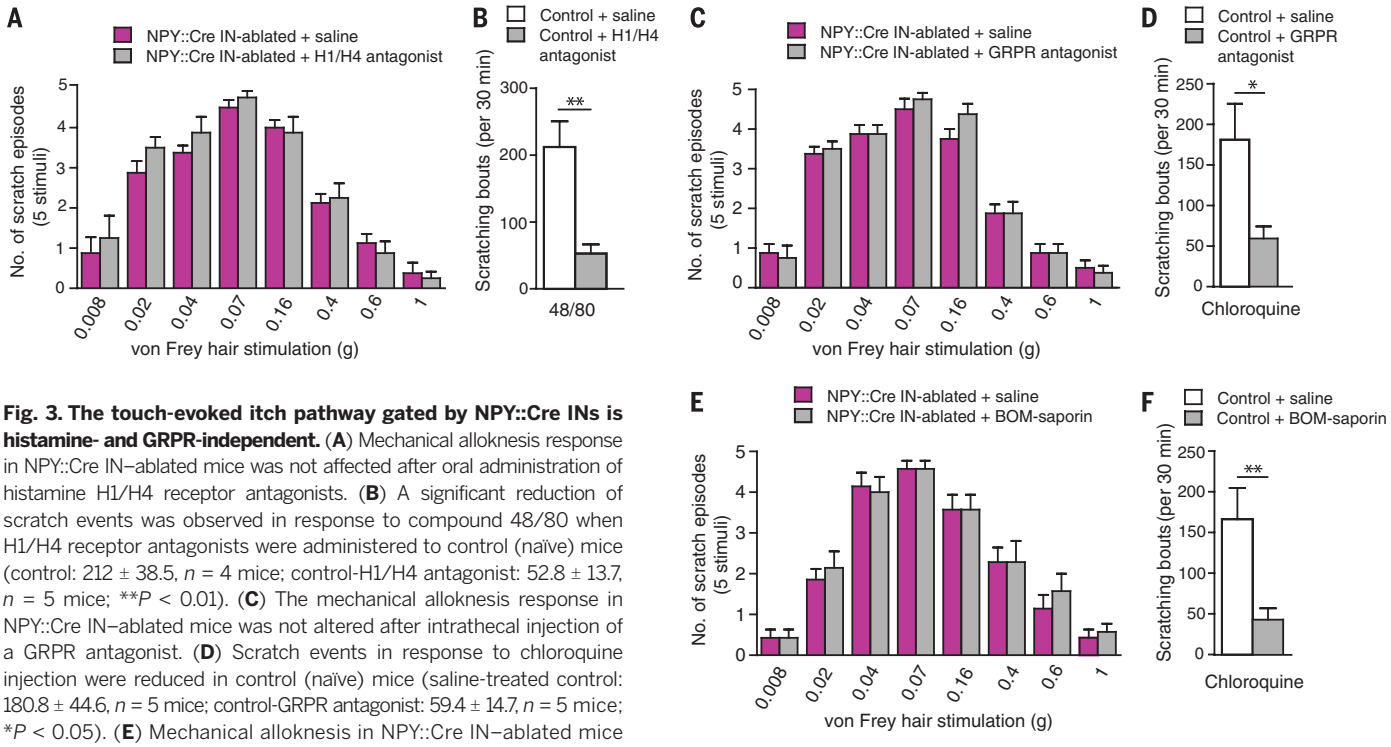

Fig. 3. The touch-evoked itch pathway gated by NPY::Cre INs is histamine- and GRPR-independent. (**A**) Mechanical alloknesis response in NPY::Cre IN–ablated mice was not affected after oral administration of histamine H1/H4 receptor antagonists. (**B**) A significant reduction of scratch events was observed in response to compound 48/80 when H1/H4 receptor antagonists were administered to control (naïve) mice (control: 212 ± 38.5, n = 4 mice; control-H1/H4 antagonist: 52.8 ± 13.7, n = 5 mice; $^{**}P < 0.01$). (**C**) The mechanical alloknesis response in NPY::Cre IN–ablated mice was not altered after intrathecal injection of a GRPR antagonist. (**D**) Scratch events in response to chloroquine injection were reduced in control (naïve) mice (saline-treated control: 180.8 ± 44.6, n = 5 mice; control-GRPR antagonist: 59.4 ± 14.7, n = 5 mice; $^{*}P < 0.05$). (**E**) Mechanical alloknesis in NPY::Cre IN–ablated mice was not affected 2 weeks after ablation of $GRPR^+$ INs in the spinal cord. (**F**) Ablation of the $GRPR^+$ INs in control (naïve) mice caused a significant reduction of scratch events induced by chloroquine injection [saline-treated control: 166.1 ± 38.5, n = 7 mice; bombesin-saporin (BOM-saporin)–treated control: 42.9 ± 13.9, n = 7 mice; $^{**}P < 0.01$]. P values were calculated using the Student's unpaired t test. Error bars indicate SEM.

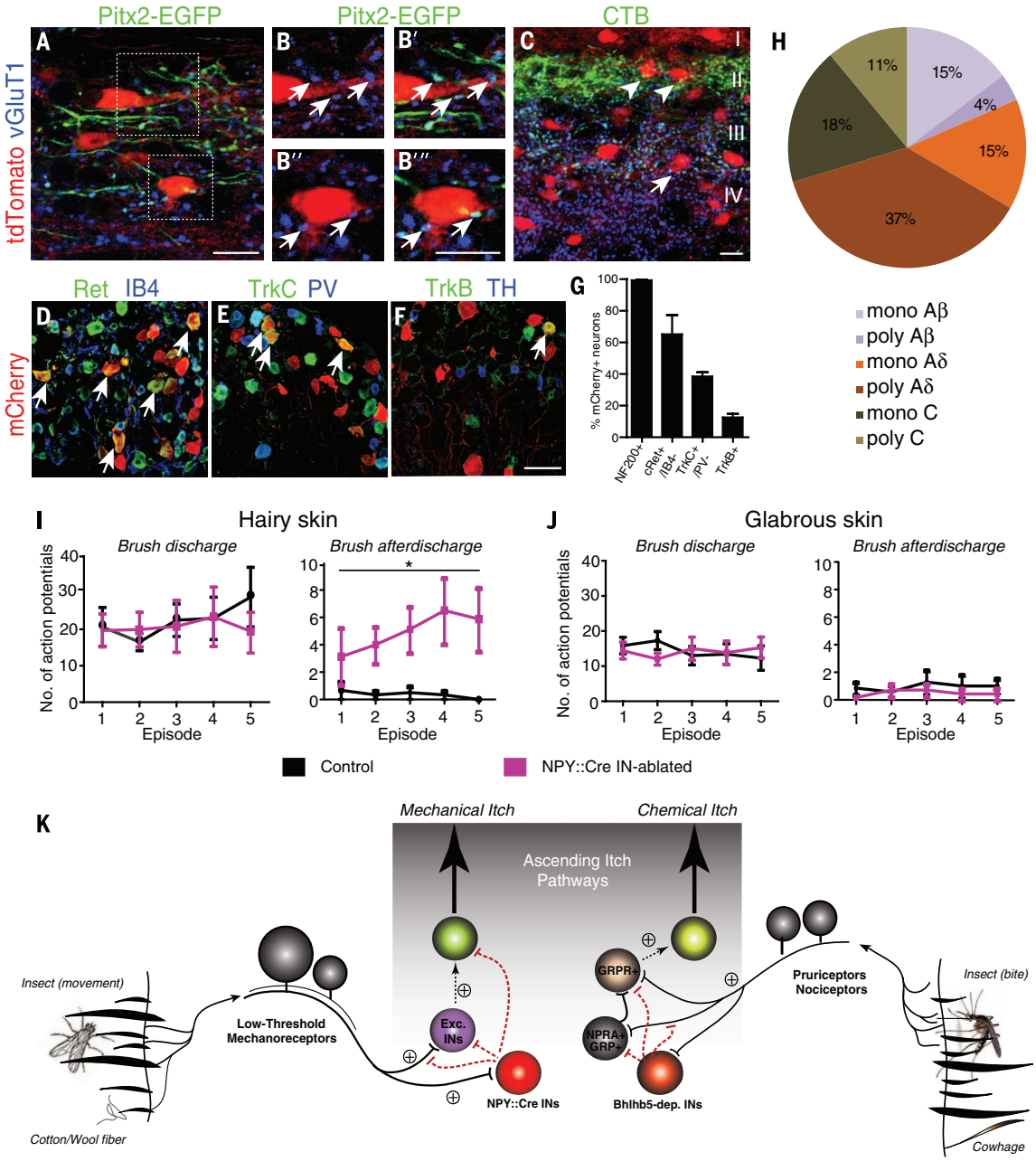

Fig. 4. NPY::Cre INs form a feedforward inhibitory pathway from hairy skin to suppress mechanical itch. (**A** to **B‴**) Sections from the lumbar dorsal spinal cord of *NPY::Cre*; *R26*$^{LSL\text{-}tdTomato}$; *Pitx2*-EGFP mice, showing Pitx2-EGFP^{+} LTM synaptic terminal afferent fibers (GFP^{+}/vGluT1^{+}) in close apposition to NPY::Cre-TdTomato^{+} INs. Higher-magnification images of the boxed areas in (A) are shown in (B) to (B‴). Arrows indicate synaptic contacts. (**C**) Sections from lumbar dorsal spinal cord of *NPY::Cre*; *R26*$^{LSL\text{-}tdTomato}$ mice 3 days after injection of CTB in hairy skin stained with the indicated markers. Arrows indicate myelinated contacts; arrowheads denote unmyelinated contacts. (**D** to **G**) Transynaptic labeling of LTMs after selective infection of NPY::Cre INs with pseudotyped EnvA-mCherry rabies virus. Shown are representative sections through the dorsal root ganglion of a P13 *NPY::Cre*; *Lbx1*^{FlpO}; *R26*$^{ds\text{-}HTB}$ mouse stained with the indicated markers of LTM subtypes [(D) to (F)]. Arrows indicate double labeled neurons. (G) Quantification of sensory neuronal markers in relation to the total number of mCherry^{+} neurons. Data: mean ± SEM; $n = 3$ mice. (**H**) Classification of potentials in NPY::Cre INs induced by dorsal root stimulation. Of the 27 recorded cells, 3 cells with a monosynaptic Aβ input displayed a second monosynaptic Aδ (1 cell) and polysynaptic C (2 cells) input. (**I** and **J**) In vivo extracellular recordings from lumbar dorsal spinal cord neurons in response to mechanical stimulation of hairy and glabrous skin. (I) Increase in the mean of afterdischarge firing of neurons with hairy-skin receptive fields in NPY::Cre IN–ablated mice compared with control mice (control: 0.4 ± 0.3 spikes/s, $n = 7$ cells; NPY::Cre IN–ablated: 4.9 ± 1.4 spikes/s, $n = 7$ cells; two-way analysis of variance, $*P = 0.03$). The number of spikes fired during active brushing was unchanged (control: 22.3 ± 4.2 spikes/s, $n = 7$ cells; NPY::Cre IN–ablated: 20.1 ± 5.7 spikes/s, $n = 7$ cells). (J) Afterdischarge firing of neurons with glabrous-skin receptive fields in NPY::Cre IN–ablated compared with control mice (control: 0.9 ± 0.3 spikes/s, $n = 5$ cells; NPY::Cre IN–ablated: 0.5 ± 0.2 spikes/s, $n = 7$ cells). The number of spikes fired during active brushing was unchanged (control: 14.1 ± 2.4 spikes/s, $n = 5$ cells; NPY::Cre IN–ablated: 15.3 ± 2.8 spikes/s, $n = 7$ cells). (**K**) Model for the mechanical itch pathway: Light-touch stimuli on hairy skin stimulates LTMs to evoke mechanical itch. This itch pathway is gated by other LTMs via their activation of inhibitory NPY::Cre INs. The mechanical itch circuit is independent of the chemical itch pathways transduced by natriuretic peptide receptor A, GRP, and GRPR (*26*), which are gated by inhibitory Bhlhb5-dependent INs. Scale bars: 10 μm [(A) to (C)]; 50 μm (F). Error bars indicate SEM [(G), (I), and (J)].

functional modules that gate different streams of somatosensory information.

In identifying a previously uncharacterized gate for low-threshold mechanical itch, this study highlights a largely overlooked driver of chronic itch—namely, the light-touch pathway that is insensitive to antihistamine or anti-GRPR drugs (*8*). Human patients with chronic itch (trichoknesis) (*25*) display a phenotype similar to that seen in the NPY::Cre IN–ablated mice. In both instances, itch sensitivity is restricted to the hairy skin. Our finding that the NPY::Cre-derived INs are innervated by tactile inputs from hairy-skin LTMs (Fig. 4) suggests that the NPY::Cre INs are key components of a spinal inhibitory circuit by which hairy-skin LTMs gate mechanical itch. We propose that the NPY::Cre INs function as rheostat for low-threshold tactile stimuli, suppressing itch and preventing excessive scratching.

REFERENCES AND NOTES

1. T. Akiyama, E. Carstens, *Neuroscience* **250**, 697–714 (2013).
2. D. M. Bautista, S. R. Wilson, M. A. Hoon, *Nat. Neurosci.* **17**, 175–182 (2014).
3. J. Braz, C. Solorzano, X. Wang, A. I. Basbaum, *Neuron* **82**, 522–536 (2014).
4. S. Davidson, G. J. Giesler, *Trends Neurosci.* **33**, 550–558 (2010).
5. L. Han, X. Dong, *Annu. Rev. Biophys.* **43**, 331–355 (2014).
6. R. H. LaMotte, X. Dong, M. Ringkamp, *Nat. Rev. Neurosci.* **15**, 19–31 (2014).
7. J. Jeffry, S. Kim, Z. F. Chen, *Physiology* **26**, 286–292 (2011).
8. M. Fukuoka, Y. Miyachi, A. Ikoma, *Pain* **154**, 897–904 (2013).
9. C. F. Wahlgren, O. Hägermark, R. Bergström, *Acta Derm. Venereol.* **71**, 488–494 (1991).
10. M. Hosogi, M. Schmelz, Y. Miyachi, A. Ikoma, *Pain* **126**, 16–23 (2006).
11. S. E. Ross *et al.*, *Neuron* **65**, 886–898 (2010).
12. E. Foster *et al.*, *Neuron* **85**, 1289–1304 (2015).
13. D. Bröhl *et al.*, *Dev. Biol.* **322**, 381–393 (2008).
14. M. Huang *et al.*, *Dev. Biol.* **322**, 394–405 (2008).
15. T. C. Sardella *et al.*, *Mol. Pain* **7**, 76 (2011).
16. S. Y. Tiong, E. Polgár, J. C. van Kralingen, M. Watanabe, A. J. Todd, *Mol. Pain* **7**, 36 (2011).
17. A. P. Kardon *et al.*, *Neuron* **82**, 573–586 (2014).
18. B. Duan *et al.*, *Cell* **159**, 1417–1432 (2014).
19. T. Akiyama *et al.*, *J. Invest. Dermatol.* **132**, 1886–1891 (2012).
20. S. G. Shimada, R. H. LaMotte, *Pain* **139**, 681–687 (2008).
21. B. N. Armbruster, X. Li, M. H. Pausch, S. Herlitze, B. L. Roth, *Proc. Natl. Acad. Sci. U.S.A.* **104**, 5163–5168 (2007).
22. Y. G. Sun, Z. F. Chen, *Nature* **448**, 700–703 (2007).
23. Y. G. Sun *et al.*, *Science* **325**, 1531–1534 (2009).
24. L. Li *et al.*, *Cell* **147**, 1615–1627 (2011).
25. A. Reich, K. Mędrek, Z. Adamski, J. C. Szepietowski, *Acta Derm. Venereol.* **93**, 591 (2013).
26. S. K. Mishra, M. A. Hoon, *Science* **340**, 968–971 (2013).

ACKNOWLEDGMENTS

This study was supported by grants from the NIH (NS086372 to M.G. and Q.M., NS080586 and NS072031 to M.G., and NS072040 to Q.M.) and by the Caterina Foundation (S.B. and S.C.K.). We thank C. Padilla and T. Velasquez for help in generating the *R26GAG*$^{ds\text{-}hM4D\text{-}tdTomato}$ mice. All data are contained in the manuscript and the supplementary materials. A.G. and E.K. were supported by the Gatsby Charitable Foundation and the NIH (grant R01 NS 067216).

SUPPLEMENTARY MATERIALS

www.sciencemag.org/content/350/6260/550/suppl/DC1
Material and Methods
Figs. S1 to S8
References (*27*–*39*)

25 June 2015; accepted 21 September 2015
10.1126/science.aac8653

BRAIN DEVELOPMENT

A GABAergic projection from the zona incerta to cortex promotes cortical neuron development

Jiadong Chen* and Arnold R. Kriegstein*

γ-Aminobutyric acid (GABA) is the major inhibitory transmitter in the mature brain but is excitatory in the developing cortex. We found that mouse zona incerta (ZI) projection neurons form a GABAergic axon plexus in neonatal cortical layer 1, making synapses with neurons in both deep and superficial layers. A similar depolarizing GABAergic plexus exists in the developing human cortex. Selectively silencing mouse ZI GABAergic neurons at birth decreased synaptic activity and apical dendritic complexity of cortical neurons. The ZI GABAergic projection becomes inhibitory with maturation and can block epileptiform activity in the adult brain. These data reveal an early-developing GABAergic projection from the ZI to cortical layer 1 that is essential for proper development of cortical neurons and balances excitation with inhibition in the adult cortex.

During embryonic development, neural activity (*1*, *2*) influences proliferation, migration, and differentiation, as well as circuit refinement (*3*–*5*). In immature brains, the neurotransmitter GABA has excitatory effects due to high intracellular chloride (*6*, *7*), contrary to its inhibitory effects in adult brains. GABA in the immature neocortex comes from local interneurons and axonal projections from other brain regions (*8*–*12*). The neonatal rodent brain has an excitatory GABAergic plexus projecting widely within cortical layer 1 (*13*, *14*). Here, we show that the zona incerta (ZI) generates the neurons of this GABAergic plexus.

We mapped the ZI pathway in transgenic mice by manipulating channelrhodopsin-2 (ChR2) expression in somatostatin (SST)–expressing neurons in the ZI of neonatal mice (postnatal day P0–P1) (*15*, *16*). Labeling was restricted to ZI GABAergic (Fig. 1A), SST$^+$ (Fig. 1C) neurons 1 week after virus injection, and we observed EYFP$^+$ ZI axonal projections widely distributed in layer 1 of somatosensory and motor cortex (Fig. 1, A and B, and fig. S1). At P7, ChR2 was reliably expressed in ZI neurons, and blue light stimulation induced firing of EYFP$^+$ ZI neurons (Fig. 1, D to F). We filled layer 5 cortical neurons with neurobiotin in acute slices of somatosensory and motor cortex and coimmunostained with the cortical layer 5 marker Ctip2 (Fig. 1I, 16/16 neurons). The apical dendrites of these pyramidal neurons contacted layer 1 EYFP$^+$ axons (Fig. 1G) and colocalized with the GABAergic presynaptic marker vGat (vesicular GABA transporter) (Fig. 1H).

Blue light stimulation of layer 1 evoked synaptic responses in layer 4 and layer 5 pyramidal neurons. The light-evoked responses were not sensitive to α-amino-3-hydroxy-5-methyl-4-isoxazole propionate (AMPA) or *N*-methyl-D-aspartate (NMDA) receptor antagonists [6-cyano-2, 3-dihydroxy-7-nitro-quinoxaline (CNQX) and D-2-amino-5-phosphonovalerate (D-APV), respectively] but were abolished by the $GABA_A$ receptor antagonist bicuculline (BMI) (Fig. 1, J to L) and reversibly blocked by tetrodotoxin (TTX, $n = 4$; Fig. 1K). Stimulation of layer 1 axons also induced GABAergic responses from layer 2/3 neurons, supporting observations that the layer 1 GABAergic plexus connects with pyramidal neurons from multiple layers in neonatal mice (*13*).

Morphologically, the human brain has abundant GABAergic synapses in cortical layer 1 as early as gestational week (GW) 12 (*17*, *18*). In the second trimester, subplate neurons show spontaneous firing and synaptic activity (*19*, *20*). Examining the expression and distribution of GABAergic axons in human cortex at GW 24, we found that both the axon marker neurofilament-2H3 and the GABAergic presynaptic marker vGat were expressed in cortical layer 1 (Fig. 2, A to C). In acute brain slices from GW 22, pyramidal neurons in deep cortical layers had high membrane resistance (1.1 ± 0.1 gigaohms, $n = 15$), low membrane capacitance (23.0 ± 2.9 pF, $n = 15$), and fired only one or two action potentials (Fig. 2, D and E) (*19*). Cortical neurons expressed $GABA_A$ receptors (fig. S2) and displayed typical GABAergic miniature synaptic currents (Fig. 2F). Thus, human cortical neurons express functional $GABA_A$ receptors and GABAergic synapses in the late second trimester.

We characterized the morphology and location of recorded cortical neurons by filling cells with neurobiotin and postimmunostaining with streptavidin-549 and the deep cortical layer marker Ctip2. Ctip2 marker expression (Fig. 2D and fig. S3) identified layer 5 pyramidal neurons with apical dendrites extending to cortical layer 1 (Fig. 2D). We recorded robust evoked synaptic responses only when stimulating layer 1 (Fig. 2G), but not deep cortical layers (−0.1 ± 0.6 pA,

Department of Neurology, Eli and Edythe Broad Center of Regeneration Medicine and Stem Cell Research, University of California, San Francisco, CA 94143, USA.
***Corresponding author. E-mail: jardongchen@gmail.com (J.C.); kriegsteina@stemcell.ucsf.edu (A.R.K.)**

Science
AAAS

Gate control of mechanical itch by a subpopulation of spinal cord interneurons

Steeve Bourane *et al.*

Science **350**, 550 (2015);
DOI: 10.1126/science.aac8653

Science (print ISSN 0036-8075; online ISSN 1095-9203) is published weekly, except the last week in December, by the American Association for the Advancement of Science, 1200 New York Avenue NW, Washington, DC 20005.